J. Membrane Biol. 15, 47–66 (1974)
© by Springer-Verlag New York Inc. 1974

Computer Simulation of Sodium Fluxes in Frog Skin Epidermis

Ernst G. Huf and John R. Howell

Departments of Physiology and Biometry, Virginia Commonwealth University, Richmond, Virginia 23219

Received 13 June 1973; revised 27 September 1973

Summary. The operation of a seven-compartment model is described with respect to flows of Na^+ within and across this system, simulating published results obtained on frog skin. The seven compartments represent: one outside and one inside solution compartment; the subcorneal space; the first reacting cell layer (1.RCL); the remaining cell compartment; the non-, or slowly exchangeable Na^+ compartment; the extracellular space. Assuming reasonable volumes for the epidermal compartments and further chosing, by trial and error, appropriate rate constants, a set of seven simultaneous linear differential equations was solved by the application of the Continuous System Modeling Program (CSMP), using an IBM 1130 computer. Initial conditions for influx, backflux and net flux were taken which correspond to $[Na^+]_0$; $[Na^+]_i = 115$ mM. Print-out data were obtained at 0.5-min intervals for 30 min, when steady states were obtained in 13 models studied, varying certain k's thus simulating actions of chemical agents (hormones; drugs). Simulation was achieved with regard to rate of influx, backflux and net flux, steady-state time (30 min), and electrical potentials. In addition, this approach gave detailed information on Na^+ pool sizes and their variations with changes in k's. These results are compared to published data on frog skin and good agreement between operation of skin epidermis and model was found.

During the last decade the three-compartment model proposed by Curran, Herrera and Flanigan [14] has frequently been used in kinetic studies of movement of ions across epithelial membranes. Some applications have recently been reviewed [38]. In this model, compartments 1 and 3 represent, respectively, the outside and the inside fluid compartments, and compartment 2 is an epithelial compartment located between two major barriers to Na^+ movement. From light- and electron-microscopic studies on frog skin epidermis [18, 19, 32–34] it would appear that in inward and outward movement of Na^+ several epithelial compartments should be considered as significant parts of a flow model. For instance, Zerahn [43] has found it useful to consider three epithelial compartments in the interpreta-

tion of Na* wash-out experiments. Multicompartmental system kinetics require knowledge of a great number of rate constants. The task of obtaining these experimentally for frog skin when considering it as a multicompartmental system is, at present at least, insurmountable. In the present study, an approach was made to describe the kinetics of Na^+ influx and Na^+ outflux by computer simulation, aiming at results which are in agreement with typical laboratory observations made on frog skin both under normal physiological conditions, and after treatment with certain hormones or drugs. Agreement was sought with respect to rates of transepithelial fluxes, steady-state time, Na^+ pools (total pool; transport pool), and epidermal electrical potentials. In this study the operation of a seven-compartment model will be discussed which closely simulates the behavior of frog skin epidermis. The results obtained, we believe, encourage new studies, both on the computer and in the laboratory, that may lead to a better understanding of the kinetics of flow of Na^+, including active Na^+ transport, in this epithelial tissue.

1. The Model

Fig. 1 shows the seven-compartment model on which this study is based. There are two external (solution) compartments (1 and 7; 5 ml each) and five internal (epidermal) compartments (2, 3, 4, 5 and 6). The latter correspond, respectively, to: 2 = subcorneal space, 0.1 μliter/cm^2; 3 = "first reacting cell layer" (1. RCL) of Voûte and Ussing [33], 0.5 μliter/cm^2; 4 = remaining epithelial cell, 4.0 μliter/cm^2; 5 = extracellular space, 0.5 μliter/cm^2; 6 = non- (or slowly) exchangeable Na^+-compartment, 0.2 μliter/cm^2. The volume figures are based on reports in the literature [1, 2, 10, 14, 16, 30, 33], except for the volume of 0.1 μliter/cm^2 for the subcorneal space which is as good an estimation as we could achieve from thickness measurements on the normal histology of skins. The volume 0.2 μliter/cm^2 for the slowly exchangeable Na^+ compartment is a fictitious figure used in two computer runs (*see* Section 3e). It will be assumed that all volumes remain constant and that the "model membrane" has an area of one cm^2 for entry of Na^+ from compartment 1, and for exit of Na^+ into compartment 7. The corium of the skin has been neglected. It constitutes a diffusion barrier of minor significance in skins of *R. pipiens* [41] (but *see* ref. [20]). A sketch approximating the essential histological appearance of the epithelium can be seen in Fig. 7 of the paper by Huf [21]. The flows between compartments 1 and 3, 3 and 4, take into consideration existing pathways between cells via cell junctions [3, 18, 19, 33]. Flow between compartments $1 \leftrightarrow 2$ may be via the cornified cells, or via the outer tight cell junctions, or via both. No distinction is

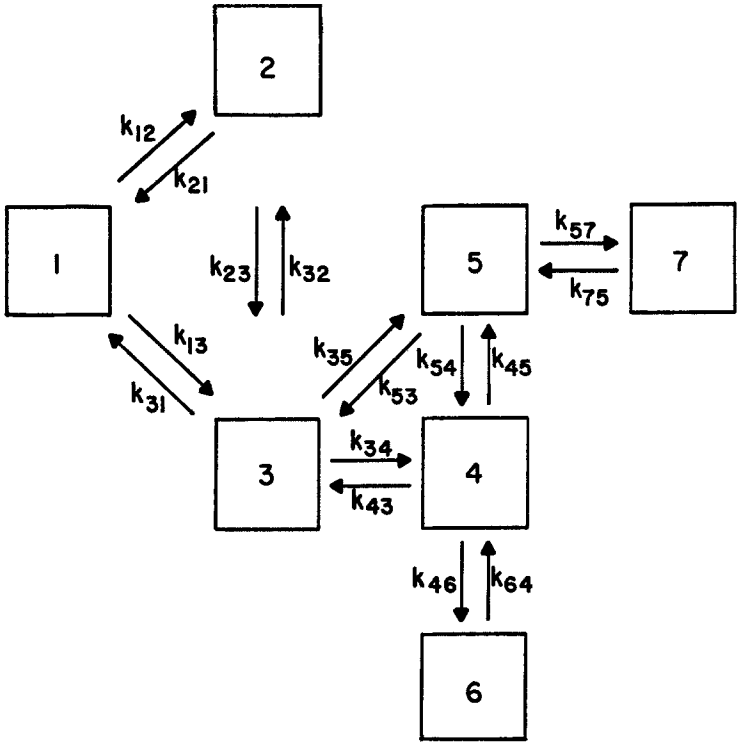

Fig. 1. The seven-compartment model, with flows between compartments defined by the rate constants k_{ij}. 1=external solution compartment. 2=subcorneal space. 3=first reacting cell layer (1. RCL). 4=remaining cell compartment. 5=extracellular space; 6=non- (slowly) exchangeable compartment. 7=internal solution compartment. Sizes for the volumes of the compartments are given in Section 1

made in the model. Pathway $2 \leftrightarrow 5$ is the pathway from the subcorneal space into the extracellular space via the inner set of tight cell junctions. In the present study it is assumed that only a negligible amount of Na^+ takes this route. Ions other than Na^+, chiefly Cl^-, K^+ or H^+, also flow through the system to preserve electroneutrality throughout. Their pathways are not considered here. Alternatively, the system may be thought short-circuited, with momentary interruption of the current for development of a membrane potential.

2. Calculations

(a) Flow Equations

The assumption is made that the flows of Na^+ can be described by first-order linear differential equations. Designating by S_j ($j=1, 2, 3, 4,$

5, 6, 7) the amount of Na^+ in a given compartment, and letting k be rate constants (coefficients), one has for the above model:

$$\frac{dS_1}{dt}=k_{21}S_2+k_{31}S_3-(k_{12}+k_{13})S_1 \tag{1}$$

$$\frac{dS_2}{dt}=k_{12}S_1+k_{32}S_3-(k_{21}+k_{23})S_2 \tag{2}$$

$$\frac{dS_3}{dt}=k_{13}S_1+k_{23}S_2+k_{43}S_4+k_{53}S_5-(k_{31}+k_{32}+k_{34}+k_{35})S_3 \tag{3}$$

$$\frac{dS_4}{dt}=k_{34}S_3+k_{54}S_5+k_{64}S_6-(k_{43}+k_{45}+k_{46})S_4 \tag{4}$$

$$\frac{dS_5}{dt}=k_{35}S_3+k_{45}S_4+k_{75}S_7-(k_{53}+k_{54}+k_{57})S_5 \tag{5}$$

$$\frac{dS_6}{dt}=k_{46}S_4-k_{64}S_6 \tag{6}$$

$$\frac{dS_7}{dt}=k_{57}S_5-k_{75}S_7. \tag{7}$$

Integration Eqs. (1) and (7) for the steady-state condition (after 30 min, *see below*) yields for S_j at 90 min ($S_{j(90)}$):

$$S_{1(90)}=\frac{k_{21}S_{2(30)}+k_{31}S_{3(30)}}{k_{12}+k_{13}} - \frac{k_{21}S_{2(30)}+k_{31}S_{3(30)}}{k_{12}+k_{13}}e^{-60(k_{12}+k_{13})}+S_{1(30)}e^{-60(k_{12}+k_{13})} \tag{8}$$

$$S_{7(90)}=\frac{k_{57}}{k_{75}}S_{5(30)}-\frac{k_{57}}{k_{75}}S_{5(30)}e^{-60k_{75}}+S_{7(30)}e^{-60k_{75}}. \tag{9}$$

Eqs. (8) and (9) were used for calculations of "transmembrane" influxes and backfluxes (outfluxes). For three cases (models 10B, 12D and 12E, *see below*) the rates of losses from compartment 1 and the gains in compartment 7, in influx experiments, were calculated. The results checked with $\pm 2\%$. Also, in backflux experiments, the rates of losses from compartment 7 agreed well with losses from this compartment calculated as influx minus

net flux. The deviations were about -1%, the latter method of calculation giving the slightly lower values.

The set of differential Eqs. (1) through (7), written in matrix form is ($\dot{S} = dS/dt$):

$$\begin{bmatrix} \dot{S}_1 \\ \dot{S}_2 \\ \dot{S}_3 \\ \dot{S}_4 \\ \dot{S}_5 \\ \dot{S}_6 \\ \dot{S}_7 \end{bmatrix} = \begin{bmatrix} -k_1 & k_{21} & k_{31} & 0 & 0 & 0 & 0 \\ k_{12} & -k_2 & k_{32} & 0 & 0 & 0 & 0 \\ k_{13} & k_{23} & -k_3 & k_{43} & k_{53} & 0 & 0 \\ 0 & 0 & k_{34} & -k_4 & k_{54} & k_{64} & 0 \\ 0 & 0 & k_{35} & k_{45} & -k_5 & 0 & k_{75} \\ 0 & 0 & 0 & k_{46} & 0 & -k_6 & 0 \\ 0 & 0 & 0 & 0 & k_{57} & 0 & -k_7 \end{bmatrix} \begin{bmatrix} S_1 \\ S_2 \\ S_3 \\ S_4 \\ S_5 \\ S_6 \\ S_7 \end{bmatrix}$$

where

$$-k_1 = -(k_{12} + k_{13}); \quad -k_2 = -(k_{21} + k_{23});$$

$$-k_3 = -(k_{31} + k_{32} + k_{34} + k_{35}); \quad -k_4 = -(k_{43} + k_{45} + k_{46});$$

$$-k_5 = -(k_{53} + k_{54} + k_{57}); \quad -k_6 = -k_{64}; \quad -k_7 = -k_{75}.$$

(b) Solutions of the Simultaneous Differential Equations

Values for S_j were estimated by computer solutions applying the Continuous System Modeling Program (CSMP). The computer used was an IBM 1130. The integration interval chosen was 0.005 min. Print-out data in seven decimals were obtained at 0.5-min intervals (k-values are expressed in min^{-1}) for a period of 30 min, which was sufficient to obtain very nearly steady states.

Fig. 2 shows the set-up diagram for the computer to solve the set of equations in the matrix.

(c) Testing for Steady State

The question whether the steady-state print-out data for the internal compartments represent true steady-state values was tested by inserting the appropriate 30-min S_j values read from the computer flow sheets into the differential Eqs. (2), (3), (4) and (5). In all cases dS_j/dt was very near to zero (0.0002 or less).

(d) Rate Constants

For most of the work compartment 6 was neglected (k_{46} and $k_{64} = 0$), except for studies described in Section 3*e*. Numerical values for the re-

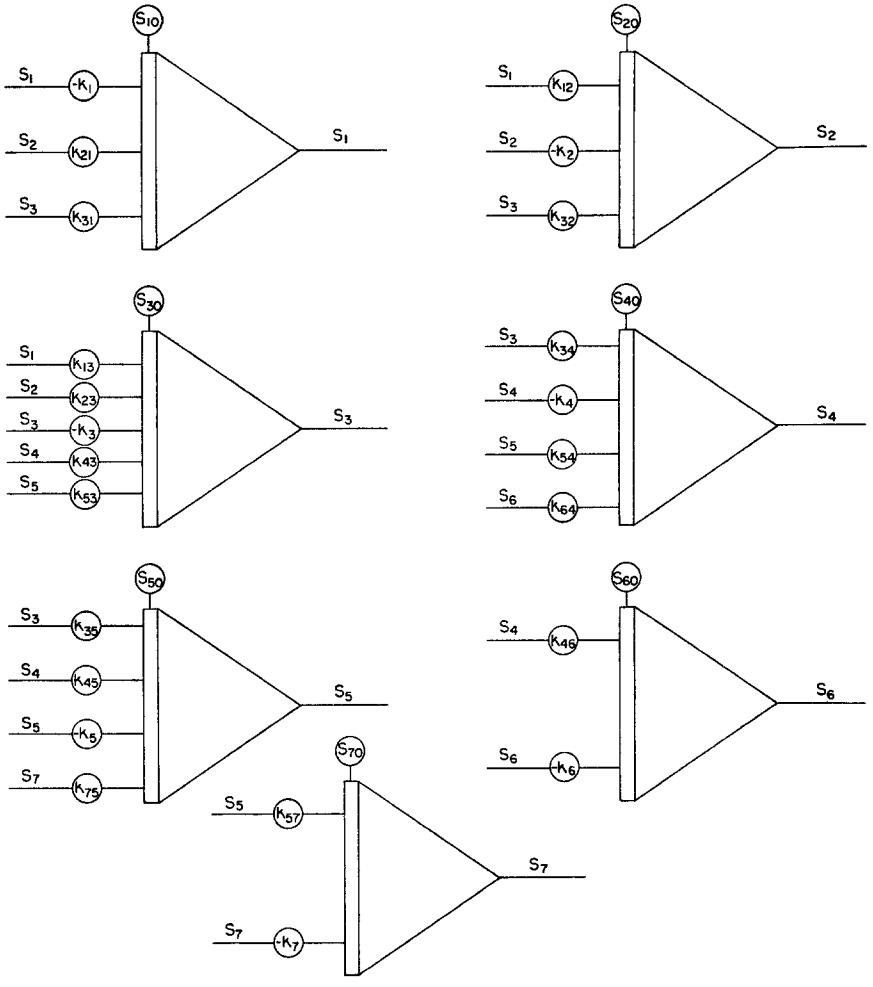

Fig. 2. Computer set-up for the seven-compartment model. The symbols represent integrators whose out-puts carry the signals which, when printed with increasing time, give the solutions to the differential equations. These out-puts are connected to the left sides of the integrators as indicated by corresponding symbols. The parameters k, and the initial conditions S are set as shown

maining 14 time-independent rate constats were chosen such that, where passive Na^+ movement occurred, a given pair of rate constants (e. g., k_{12} and k_{21}) were in proportion inversely related to the volumes of the two compartments involved, applying the relationship: $k = A \cdot P/V$ (e. g., $k_{12} = A \cdot P/V_1$, and $k_{21} = A \cdot P/V_2$). A is the area of the barrier between compartments 1 and 2, with apparent permeability coefficient P. For reasons given in a previous paper [30] we were interested in modeling the system such that "strong Na^+ pumps" operate between compartments 3 and 5, and "weak Na^+

Table 1. Rate constants (min^{-1})[a]

Model	10^5k_{12}	k_{21}	10^5k_{13}	k_{31}	k_{35}	k_{45}	10^5k_{46}	10^3k_{64}	k_{57}	10^4k_{75}
10B	2	1	2	0.2	10	0.5	0	0	4	4
10C	4	2	2	0.2	10	0.5	0	0	4	4
10D	8	4	2	0.2	10	0.5	0	0	4	4
10E	16	8	2	0.2	10	0.5	0	0	4	4
10Ea	16	8	2	0.2	10	0.5	0	0	12	12
10Eb	16	8	2	0.2	10	0.5	5	1	4	4
11C	2	1	4	0.4	10	0.5	0	0	4	4
11D	2	1	8	0.8	10	0.5	0	0	4	4
11E	2	1	16	1.6	10	0.5	0	0	4	4
12D	2	1	2	0.2	1.25	0.5	0	0	4	4
12E	2	1	2	0.2	0.625	0.5	0	0	4	4
12F	2	1	2	0.2	0.3125	0.5	0	0	4	4
12G	2	1	2	0.2	0.1	0.25	0	0	4	4

[a] The following rate constants were the same for all models: $k_{23}=1.0$; $k_{32}=0.2$; $k_{34}=0.04$; $k_{43}=0.005$; $k_{53}=0.1$; $k_{54}=2.0$.

pumps" operate between compartments 4 and 5. Therefore, the above $k-V$ relationship was not applied here. Relatively large rate constants (k_{35} and k_{45}) were chosen to express Na^+ pumping activity. Here as well as in selecting all other rate constants, a few trials guided us to achieve the aims mentioned in the Introduction. All rate constants are expressed in min^{-1}. Table 1 summarizes the rate constants used in this study, modeling thirteen specific cases with variations of k-values.

As a starting point in selecting the needed rate constants, we took the k_{12} value given by Cereijido, Herrera, Flanigan and Curran [10] as 0.000167 min^{-1} for skin area 3.14 cm^2 and outside fluid volume $V_1 = 5.0$ ml. Curran, Herrera and Flanigan [14] have given approximate values for the thickness of the cellular transport compartment, from which it can be estimated that the volume of this compartment (speaking in terms of their 3-compartment model) $V_2 = 14.8$ µliter/3.14 cm^2 (4.7 µliter/cm^2). Applying $k_{21} = k_{12} \cdot V_1/V_2$, a value of 0.06 min^{-1} is obtained, which is nearly the value actually found by these authors; i. e., $k_{21} = 0.07$ min^{-1}. With this information we set out to bring all rate constants needed for the operation of the model shown in Fig. 1 into such relation to each other as to achieve close simulation of the Na^+ transport characteristics of frog skin epidermis. The models of the 10-series (Table 1), and among them especially 10E which will emerge as the most fitting one must be considered as but one of several possible solutions. The chosen values for the rate constants, of course, must be experimentally tested before uniqueness of this model can be claimed.

(e) Initial Conditions

Computer experiments were carried out to give data on "transmembrane" flux rates for influx, backflux and, in seven cases, net flux. For influx, the initial condition was $S_1 = 575$ units in compartment 1. All other compartments were empty at time zero. Similarly for backflux, the initial condition was $S_7 = 575$ units in compartment 7, all other compartments being empty at time zero. In net flux experiments, initial conditions were S_1 and $S_7 = 575$ units in compartments 1 and 7, all other compartments empty at zero time.

(f) Na^+ *Pools*

To give the number $S_1(S_7) = 575$ chemical meaning we define: A print-out number of 1.0000000 represents 1 μEquiv Na^+. Thus, all S_j print-out numbers on the computer flow sheets give the sizes of the Na^+ pools (μEquiv). We further define:

$S_{ji}(S_{jb})$ = effective Na^+ pool in compartment j in influx (backflux);

$S_{jn} = (S_{ji} + S_{jb})$ = Na^+ pool in compartment j in net flux;

$S_{ji}/S_{jn}(S_{jb}/S_{jn})$ = effective Na^+ pool fraction in compartment j in influx (backflux);

$\Sigma S_{ji} = P_i(\Sigma S_{jb} = P_b)$ = combined effective Na^+ pools in all compartments in influx (backflux);

$\Sigma S_{jn} = P_i + P_b = P_n$ = total Na^+ pool in all compartments in net flux.

$P_i/P_n(P_b/P_n)$ = combined effective pool fractions in influx (backflux). In six of the 13 models studied, only influx and outflux (no net flux) experiments were carried out to save computer time. In the remaining seven cases, net fluxes were also run. It turned out that the S_{jn} so obtained agreed within $\pm 0.01\%$ (S_2; S_3), and $\pm 0.02\%$ (S_4; S_5) with the values calculated as $(S_{ji} + S_{jb})$.

(g) Calculation of the $[Na^+]$ *in the Compartments*

By the definition given in Section 2*f* and the assumed volumes of the compartments (Section 1), the $[Na^+]$ in the compartments was calculated. For example, compartments 1 and 7 (at time zero): 575 μEquiv/5 ml = 115 mM. This was also done for obtaining $[Na^+]$ in the internal compartments in steady state in net flux experiments. For example, when in compartments 3 (0.5 μliter) the print-out result was $S_{3n} = 0.0372698$ μEquiv, its $[Na^+]$ was 74.54 mM.

(h) Flux Rates

This is best explained by example. In model 10E (influx) the print-out data for calculation of "transmembrane" influx using Eq. (9) were: $S_{5\,(30)} = 0.0052774$, $S_{7\,(30)} = 0.5972704$; $k_{75} = 4.0$, $k_{57}/k_{75} = 10{,}000$. By calculation then, $S_{7\,(90)} = 1.8346$ (rounded off). The increment in S_7/hr, therefore, is $1.8346 - 0.5973 = 1.2373$ (print-out number). This is equivalent to $J_i = 1.2373$ μEquiv $Na^+ \times hr^{-1} \times cm^{-2}$ since by definition the number "1" stands for one μEquiv Na^+, and the exit barrier from 5 to 7 is taken as 1 cm^2. Values for backflux (J_b) and net flux (J_n) were calculated in the same way.

Steady-state flux rates were also calculated directly by using the print-out data on the computer flow sheets, e. g., those for time 25 and 30 min. When this was done for gains in the sink compartment (7 in influx, and 1 in backflux) the results agreed within $\pm 1\%$ with those calculated by using Eqs. (8) or (9). This method of flux calculation failed when it was applied to losses in the source compartment (1 in influx and 7 in backflux) because, here, one calculates small differences of large numbers which are afflicted with errors attributable, probably, to the great imbalance in the magnitude of the k values of the system.

(i) Initial Rates of Loading of Internal Compartments (J_L)

The print-out data for the internal compartments (2, 3, 4, 5) for the first 30 sec were expressed as μequivalents Na^+ as described in Section 2*f*. The results were summed up and multiplied by 120. Thus, a value for J_L in μEquiv $\times hr^{-1} \times cm^{-2}$ was obtained, assuming that this rate had been kept constant for 1 hr. Then a comparison was made between J_L and J_n.

(j) Epithelial Electrical Potentials

The equation $V_{23} = 58 \log [Na^+]_2/[Na^+]_3$ was applied in which V_{23} is the potential across the barrier between compartments 2 and 3 (subcorneal space and 1. RCL). This barrier is assumed to be Na^+ permselective [24].

3. Results

(a) Na^+ *Pools*

Protocols for six model experiments are presented in Table 2. By the definition given in Section 2*f*, these figures give the Na^+ pool sizes S_j in

Table 2. Examples of 30-min print-out data obtained in six models in near steady state[a]

	Model	10B	10E	10Ea	11D	12F	12G
Influx	S_{2i}	0.0059132	0.0102548	0.0102539	0.0062182	0.0084315	0.0097120
		(98.89)	(99.86)	(99.86)	(99.00)	(89.00)	(84.60)
	S_{3i}	0.0017149	0.0021428	0.0021028	0.0048475	0.0268585	0.0396632
		(72.06)	(76.45)	(76.10)	(88.54)	(72.06)	(69.17)
	S_{4i}	0.0168488	0.0210539	0.0072870	0.0476368	0.0113000	0.0165748
		(6.90)	(8.48)	(3.10)	(17.35)	(4.78)	(3.63)
	S_{5i}	0.0042233	0.0052774	0.0018019	0.0119393	0.0023182	0.0013377
		(6.86)	(8.42)	(3.04)	(17.25)	(3.93)	(2.34)
	$P_i=\Sigma S_{ji}$	0.0287002	0.0387289	0.0214456	0.0706418	0.0489082	0.0672877
	P_i/P_n%	9.136	11.952	6.986	19.866	14.292	11.553
Backflux	S_{2b}	0.0000666	0.0000148	0.0000148	0.0000629	0.0010419	0.0017685
		(1.11)	(0.14)	(0.14)	(1.00)	(11.00)	(15.40)
	S_{3b}	0.0006649	0.0006599	0.0006603	0.0006276	0.0104113	0.0176814
		(27.94)	(23.55)	(23.90)	(11.46)	(27.94)	(30.83)
	S_{4b}	0.2273210	0.2272713	0.2274375	0.2269568	0.2251906	0.4397371
		(93.10)	(91.52)	(96.90)	(82.65)	(95.22)	(96.37)
	S_{5b}	0.0573866	0.0573742	0.0574148	0.0572954	0.0566540	0.0559581
		(93.14)	(91.58)	(96.96)	(82.75)	(96.07)	(97.66)
	$P_b=\Sigma S_{jb}$	0.2854391	0.2853202	0.2855274	0.2849427	0.2932978	0.5151451
	P_b/P_n%	90.864	88.048	93.014	80.134	85.708	88.447
Net flux	S_{2n}	0.0059798	0.0102696	0.0102687	0.0062811	0.0094734	0.0114805
	S_{3n}	0.0023798	0.0028027	0.0027631	0.0054751	0.0372698	0.0573446
	S_{4n}	0.2441698	0.2483252	0.2347245	0.2745936	0.2364906	0.4563119
	S_{5n}	0.0616099	0.0626516	0.0592167	0.0692347	0.0589722	0.0572958
	$P_n=\Sigma S_{jn}$	0.3141393	0.3240491	0.3069730	0.3555845	0.3422060	0.5824328

[a] $S_j=Na^+$ pool, subscripts i, b, n refer to influx, backflux, net flux condition. The figures in parentheses are values for pool fractions: $100\,S_{ji}/S_{jn}$ and $100\,S_{jb}/S_{jn}$.

μequivalents. In all cases (including those for which protocols are omitted) the pool fractions for compartments 2 and 3 are much greater than the pool fractions in 4 and 5 during steady-state influx. The reverse is true during backflux. The same is found if one compares the values for combined effective pool fractions (100 P_i/P_n, 100 P_b/P_n, Table 2). This is not unexpected. In a multicompartment system, such as considered here, the internal membrane compartments nearest the higher external Na^+ pool are likely to have higher pool fractions than those nearer the external compartment with the lower Na^+ pool. Numerical values for pool sizes and pool fractions for given sets of k's could not have been conveniently obtained without the use of the computer.

A corollary of this is the following: If with initial conditions $S_1 = S_7 =$ 575 μEquiv Na^+, separate influx and backflux studies were done by adding equal amounts of radiosodium (Na*) to the outside (specific activity σ_1), or the inside (σ_7), respectively, the steady-state Na* pools (S_j^*) would be in proportion to each other as given by the percent figures in Table 2. Full labeling, $S_{jn}^*/S_{jn} = \sigma_{jn}$, would occur when both compartments 1 and 7 contained equal amounts of Na* ($\sigma_{jn} = \sigma_1 = \sigma_7$). For steady-state Na* influx, $\sigma_{ji} = S_{ji}^*/S_{jn} = f_{ji}\sigma_1$; for Na^+ backflux, $\sigma_{jb} = S_{jb}^*/S_{jn} = f_{jb}\sigma_7$, where the f's are the percent figures in Table 2. For example, in model 10E, $\sigma_{2i} = 99.86\%\ \sigma_1$; or $\sigma_{2b} = 0.14\%\ \sigma_7$.

Space does not permit us to describe in detail the results contained in Table 2. Attention should be focussed at the changes in pool sizes with changing k's.

Table 3. Percent values for steady-state Na^+ pool sizes, relative to total Na^+ pool $S_{jn} = 100$ in model 12G in which no Na^+ pumps are operating

	Model	10B	10E	10Ea	11D	12F	12G
Influx	S_{2i}	51.51	89.32	89.32	54.16	73.44	84.60
	S_{3i}	2.99	3.74	3.67	8.46	46.83	69.17
	S_{4i}	3.69	4.61	1.60	10.44	2.48	3.63
	S_{5i}	7.37	9.21	3.15	20.84	4.05	2.34
Backflux	S_{2b}	0.58	0.13	0.13	0.55	9.08	15.40
	S_{3b}	1.16	1.15	1.15	1.09	18.16	30.83
	S_{4b}	49.82	49.81	49.84	49.74	49.35	96.37
	S_{5b}	100.16	100.14	100.20	100.00	98.88	97.66
Net flux	S_{2n}	52.09	89.45	89.45	54.71	82.52	100.00
	S_{3n}	4.15	4.89	4.82	9.55	64.99	100.00
	S_{4n}	53.51	54.42	51.44	60.18	51.83	100.00
	S_{5n}	107.53	109.35	103.35	120.84	102.93	100.00
	P_n	53.94	55.64	52.71	61.05	58.76	100.00

We thought it of interest to compare the Na^+ pumping models (10B, 10E, 10Ea, 11D and 12F) with the nonpumping model (12G). The S_{jn} pools in model 12G were set equal to 100, and the percent pool values for the other models were calculated using the data in Table 2. For example, for model 10B, $S_{2i} = 100 \times 0.0059132/0.0114805 = 51.5\,\%$ of S_{2n}, model 12G. The results of these calculations are shown in Table 3.

(b) $[Na^+]$ *in Compartments. Transmembrane Flux Rates. Rates of Loading.* V_{23}

Table 4 gives the calculated results on $[Na^+]_j$, J_i, J_b, J_n and J_L as explained in Sections 2*g*, *h*, *i* and *j*. Data are included, here, applying to models for which protocols are omitted from Table 2.

(c) Na^+ *Fluxes Between Compartments*

The k values in Table 1 and the S_j data in Table 2 were used to calculate rates for influx, backflux, and net flux of Na^+ between compartments. Values for net fluxes are given in Fig. 3, for models 12G and 10E. The total box sizes represent S_{jn}, the shaded areas the pool fractions (Table 2) S_{ji}/S_{jn} (influx), and S_{jb}/S_{jn} (backflux). The discrepancy between J_{54} and J_{43} (12G) may be explainable on the basis that compartment 4 was not as nearly in steady-state as others. If S_{4b} would be 0.44 % greater than the print-out value, then $J_{54} = 0.09$, with insignificant increase in J_{43}. 12G is in near perfect diffusion equilibrium; $J_i = J_b = 0.32$ μEquiv $\times$ $cm^{-2} \times hr^{-1}$. The small discrepancy noted ($J_{75} = 0.35$) could be accounted for by a similar argument as presented above, applied to compartment 5. In the appendix of the paper that follows immediately we have tested for computational errors involved, which also contribute to the discrepancies noted in some of the figures shown in Fig. 3. Summation of fluxes between compartments is satisfactory [e. g., in influx $(J_{13} + J_{23}) = (J_{34} + J_{35})$]. In model 10E (with pumps), $J_i = 1.25$, $J_b = 0.015$ μEquiv $\times$ $cm^{-2} \times hr^{-1}$. A very small amount of Na^+, $100 \times 0.0015/1.25 = 0.12\,\%$ recirculates between compartments $3 \rightarrow 5 \rightarrow 4 \rightarrow 3$ during influx. 99.88 % of the Na^+ passing the main pump from $3 \rightarrow 5$ is Na^+ that comes from external compartment 1. In backflux, $100 \times 0.052/0.067 = 77.6\,\%$ Na^+ recirculates between $3 \rightarrow 5 \rightarrow 4 \rightarrow 3$, and 0.015 μEquiv $\times$ $cm^{-2} \times hr^{-1}$ (22.4 %) escapes into compartment 1. In net flux condition ($S_1 = S_7 =$ 575 μEquiv Na^+) the fraction of recirculating Na^+ was calculated as 5.1 % of a net flow of 1.305 μEquiv $\times$ $cm^{-2} \times hr^{-1}$ via the pump $3 \rightarrow 5$ under these conditions.

Table 4. Steady-state values for $[Na^+]_j$, mM. Rates of transmembrane influx (J_i), backflux (J_b), net flux (J_n), and initial rate of loading (J_L), $\mu Equiv \times cm^{-2} \times hr^{-1}$. Na^+ diffusion potential V_{23}, mV

Model No.	$[Na^+]_2$	$[Na^+]_3$	$[Na^+]_4$	$[Na^+]_5$	J_i	J_b	J_n	$\%J_b/J_i$	J_L	J_L/J_n	V_{23}[b]
10B	59.80	4.76	61.04	123.22	0.996	0.012	0.984	1.23	0.980	0.99	+63.7
10C	78.26	5.12	61.49	124.12	1.097	0.013	1.084	1.19	1.325	1.22	+68.7
10D	92.95	5.41	61.85	124.83	1.181	0.014	1.167	1.19	1.710	1.47	+71.6
10E	102.70	5.61	62.08	125.30	1.237	0.015	1.222	1.20	1.989	1.63	+73.3
10Ea	102.69	5.53	58.68	118.43	1.209	0.015	1.194	1.24	1.733	1.45	+73.6
11C	60.87	6.91	63.68	128.52	1.618	0.016	1.602	0.99	1.413	0.88	+54.8
11D	62.81	10.95	68.65	138.47	2.800	0.034	2.766	1.20	2.237	0.81	+44.0
11E	66.34	18.18	77.53	156.27	4.911	0.059	4.852	1.20	3.736	0.77	+32.6
12D	72.87	30.83	59.04	121.25	0.829	0.077	0.752	9.26	1.148	1.53	+21.7
12E	82.77	50.62	59.78	119.75	0.705	0.126	0.579	17.83	1.177	2.03	+12.4
12F	94.73	74.54	59.12	117.94	0.544	0.185	0.359	34.06	1.194	3.33	+ 6.0
12G	114.81	114.69	114.08	114.59	0.320[a]	0.346[a]			1.206		+ 0.03

[a] For a possible explanation of the small discrepancy, *see* Results, Section *c*. A computer run for initial conditions $S_1 = S_7 = 575$ μEquiv Na^+ showed $J_n = 0.0002$ $\mu Equiv \times cm^{-2} \times hr^{-1}$ Na^+ lost from compartment 1.

[b] $V_{23} = (\phi_3 - \phi_2)$.

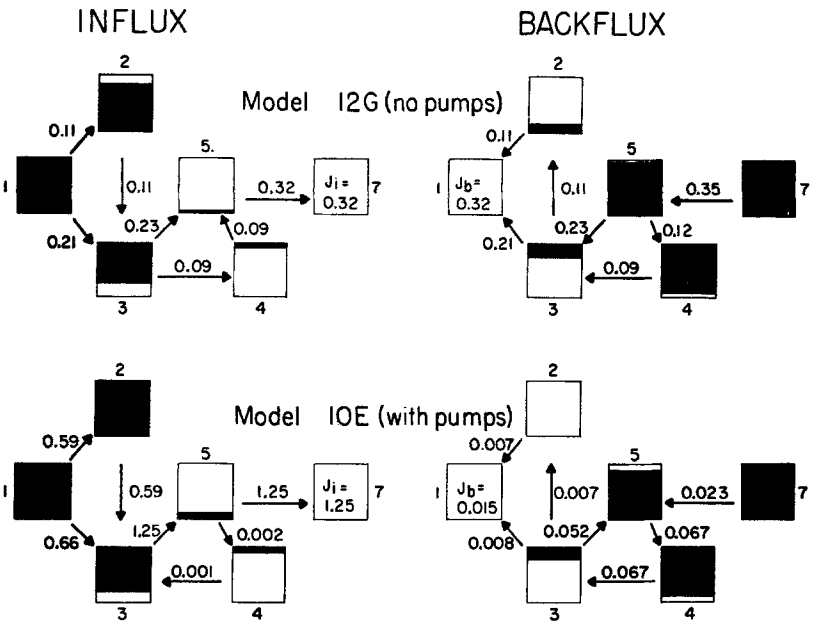

Fig. 3. Na-pools and effective pool fractions for models 12G and 10E, in steady state. The numbers at the arrows give rates for net fluxes between compartments. The slowly exchangeable compartment 6 is omitted in this case. No Na^+ pumps operate in 12G. In 10E "strong" and "weak" Na^+ pumps operate from $3 \rightarrow 5$, and $4 \rightarrow 5$, respectively. The effective pool in compartment 2 (10E, backflux) was too small to be shown in the illustration. (*See* Table 2)

(d) Time Course of Reaching Steady State

This is illustrated in Fig. 4 which was constructed for model 10E from the print-out flow sheet data. $[Na^+]$ was calculated as explained in Section 2*g*. Near steady state in all compartments is reached in about 20 min. With initial conditions $S_1 = S_7 = 575$ μEquiv Na^+, all other compartments empty at zero time (Fig. 4*C*), it is seen, as expected, that $[Na^+]_7$ first decreases, then rises again, because of net Na^+ transport $1 \rightarrow 7$. $[Na^+]_1$ continuously decreases. Once steady state is reached, $\Delta[Na^+]_1 = \Delta[Na^+]_7$ $J_n = 1.222$ μEquiv $\times$ $cm^{-2} \times hr^{-1}$.

(e) The Slowly Exchangeable Na^+ *Compartment 6*

The parameters used in this model, 10Eb, were the same as those used in 10E, except that compartment 6 ($V_6 = 0.2$ μliter/cm^2, $S_6 = 0.1242$ μEquiv Na^+) was connected to compartment 4 (Fig. 1), with rate constants $k_{46} = 0.00005$ and $k_{64} = 0.001$. Since the total (rapidly) exchangeable Na^+

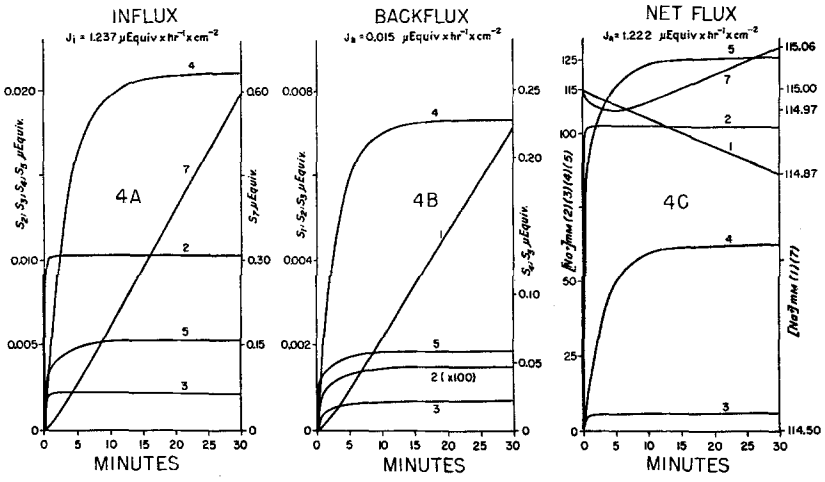

Fig. 4. Steady-state build-up of Na^+ pools, $[Na^+]$, and transmembrane flux rates in 10E. *Ordinate*: Pool sizes, S_j, in influx (4*A*); backflux (4*B*); $[Na^+]$ (4*C*). *Abscissa*: time in minutes

pool in 10E, $P_n = 0.3240491$ μEquiv Na^+ (Table 2), the addition of compartment 6 represents recognition of the presence of 38% of the total Na^+ pool ($P_n + S_6$) as slowly exchangeable Na^+. Two computer runs were done: First, with initial conditions in compartments 1, 2, 3, 4, 5 and 7 as read from the 30-min flow sheet in 10E, net, when 10E was in near steady state, but with S_6 added to it. In this study $J_n = 1.227$, as compared to $J_n =$ 1.222 μEquiv $Na^+ \times cm^{-2} \times hr^{-1}$ (10E without 6, Table 4). Thus, the Na^+ in compartment 6 contributes little to J_n. Second, with initial conditions $S_1 = S_7 = 575$ μEquiv Na^+, all other compartments including 6 empty at zero time. After 30 min compartment 6 contains only 0.26% of its assumed maximal value (0.1242), whereas by that time all other internal compartments are 100% filled. No studies were done with other k_{46} and k_{64} values.

4. Discussion

(a) Na^+ *Pools*

By employing the skin slicing method of Hvid-Hansen and Zerahn [23], Cereijido, Reisin and Rotunno [11] found 0.079 μEquiv Na^+/μliter epidermal (*Leptodactylus ocellatus*, *L.*, $[Na^+]_0 = [Na^+]_i = 115$ mM). This would give a total Na^+ pool of 0.419 μEquiv/cm^2, assuming an epidermal volume of 5.3 μliter/cm^2 (*see* Section 1). 25% of this Na^+ is not, or only slowly exchangeable with Na*. Comparable results for skins of *R. esculenta* and *R.*

pipiens were obtained by Nagel and Dörge [25, 26], Dörge and Nagel [16] and Aceves and Erlij [1]. These authors agree in that only 10 to 12% of the exchangeable Na^+ exchanges with Na* from the outside. This fraction is taken as the active Na^+ transport pool. A much higher fraction of epidermal Na^+ exchanges when Na* is placed on the inside of the skin.

In model 10Eb a total of 0.448 μEquiv Na^+/cm^2 was chosen, and 38% of it was considered slowly exchangeable; its presence did not significantly change J_n. Table 2 shows that in all models (including those omitted from protocol presentation) the Na^+ pool fraction in influx (7 to 20%) is smaller than the pool fraction in outflux (93 to 80%). This also holds for 12G where no Na^+ pumps are operating. The experimental data on skin epidermis referred to above, therefore, may be considered as a strong argument in favor of involvement of several compartments within the epidermis, as is also evidenced by its fine structure. Earlier work from this laboratory [22, 40] had led us to conclude that there must be compartmentalized functions in the handling of Na^+ and K^+ metabolism in skin epidermis: one concerned with "maintenance electrolyte equilibrium", another with "unidirectional active ion transport". The analysis of the electrical response of the outer border of skin to changes in $[Na^+]_0$ supports this view [30].

Several papers have appeared in the literature dealing with correlations between Na^+ pool size and rates of Na^+ fluxes across the skin subjected to various treatments. Increases in fluxes associated with increases in pool size were seen when applying ADH which increases the Na^+ permeability of the outer border [13, 14, 43]. Models 10E and 11D, compared to 10B (Tables 2, 3 and 4) simulate these effects. In 10E, S_2 is more affected than S_3, S_4, or S_5. The reverse is the case in 11D. S_2 may be considered as the pretransport pool, S_3 the transport pool proper.

Similar considerations may be applied to the data on the effects of amiloride on frog skin [16, 29]. It decreases J_n, but has little effect on the intracellular Na^+ pool which is exchangeable from the corium side. The Na^+ pool which is exchangeable from the epithelial side is diminished. The model results (10B *vs.* 10E and 11D) are in agreement with these findings. Zerahn [43] found that ouabain which is often said to specifically inhibit the Na^+ pump, as does fluroacetate [22] decreases J_n and greatly increases the total Na^+ pool. This has been confirmed by Nagel and Dörge [26], and by Aceves and Erlij [1] except that these authors do not find the pool changed because of more Na^+ entering from the outside. Models 12F and especially, 12G (no pump action) when compared to 10B, simulate this Na^+ accumulation in the system (Tables 2 and 3). Cereijido and Rotunno [13] and Aceves and Erlij [1] have pointed out that a drug may have more than one site of

action. Secondary volume changes of compartments may also occur. This as well as animal species differences could explain discrepancies in experimental findings. In the present model studies, a basic assumption is that volume changes do not occur. This restriction could be removed.

(b) Steady-State $[Na^+]$ *in Compartments*

In all models, except 12G (no Na^+ pumps), $[Na^+]_2 > [Na^+]_3$. This allows for passive entry of Na^+ into the main active Na^+ transport compartment in agreement with the hypothesis developed for skin by Koefoed-Johnson and Ussing [24]. In the remaining cell compartment, $[Na^+]_4 > [Na^+]_3$, except in models 12F and 12G. While this $[Na^+]$ profile is maintained in steady state, some Na^+ recirculates between certain compartments. From the data in Section 3*c* it can be calculated that in the backflux condition ($S_1 = 0$; $S_7 = 575$ μEquiv Na^+) the Na^+ which recirculates through the pump $3 \rightarrow 5$ constitutes only 4% ($0.052 \times 100/1.305$) of the net flow of Na^+ via $3 \rightarrow 5$ in the net flux condition ($S_1 = S_7 = 575$ μEquiv Na^+). This correlates well with data on oxygen consumption of skins in solutions of low *vs.* high $[Na^+]_0$ [42]. In all Na^+ pumping models, $[Na^+]_5$ (extracellular space) is greater than $[Na^+]$ in the external solutions, a feature which is in agreement with the views held by Diamond and Bossert [15]. Steady-state time for all 13 models is approximately 20 min. It is common experience that it takes no more than 30 min to obtain stable flux rates in frog skin.

(c) Transmembrane Fluxes

The models 10B–12F give values for J_i and J_b (Table 4) varying with conditions from 0.36 to 4.95, and 0.19 to 0.01 μEquiv $\times$ $cm^{-2} \times hr^{-1}$, respectively. These are the ranges found for skins by most investigators. Skin and models behave in much the same manner when comparing changes in fluxes resulting from well known influences of hormones and drugs: e. g., ADH (stimulatory; amiloride (inhibitory); catecholamines (stimulatory or inhibitory depending on experimental conditions [35, 36]); ouabain (inhibitory). Decrease in Na^+ influx associated with increase in backflux (12 series) was observed by Biber, Chez and Curran [5] in ouabain-treated skins. Decrease in influx associated with decrease in backflux (10 and 11 series) was noted by Salako and Smith [28] in skins treated with amiloride. Increase and decrease in Na^+ influx with no clear-cut changes in Na^+ outflux was recently described by Huf [21], suggesting more separate pathways. To account for this, the model requires certain changes. (Pathway $2 \leftrightarrow 5$?)

(d) Initial Rates of Uptake of Na^+

Rotunno, Villalonga, Fernandez and Cereijido [27], Biber and Curran [7], Biber [4], and Biber, Cruz and Curran [6] have shown that in skins of *R. pipiens* and *Leptodactylus ocellatus, L.*, the initial rate of uptake of Na^+ from the epidermal side (J_L) is 3 to 6 times greater than the rate of transmembrane net Na^+ flux. Ouabain had no effect on J_L when $[Na^+]_0$ was 115 mM. But since this drug inhibits net flux rate (J_n), the J_L/J_n ratio greatly increases. The 10 and 12 series models show the same trend, except that the J_L/J_n values are much smaller than found in skin. This and the fact that the increase in J_L/J_n seen in skins treated with amiloride [7], and the decrease in J_L/J_i seen when using ADH [13] is the opposite to what the model shows, points to a discrepancy between behavior of skin and model. We suspect involvement of an additional (8th) compartment which is directly connected to the outside compartment 1, such as the glands in the skin which respond to many chemical agents [8, 37].

(e) Na^+ *Diffusion Potential,* V_{23}

If the border between compartments 2 and 3 (subcorneal space/1.RCL) is perfectly Na^+-permselective [24], the Na^+ diffusion potentials as given in Table 4 (10, 11 series) could arise. The calculated values are in fair agreement with those measured by microelectrode puncture studies in "open" skins [9, 17, 31, 39]. The value of 73 mV in model 10E does seem a bit high, compared to data in the literature. But a closer comparison is difficult because this should perhaps include consideration of the associated transmembrane fluxes on which the pertinent literature is sparse. Application of the Nernst equation probably is an oversimplification.

Appendix

The matrix formulation of the differential equations presents a simple algorithm for writing them by inspection of the compartment model. If in the model one labels an arrow from compartment i to compartment j as k_{ij}, then the coefficient matrix of k values may be constructed in the following manner: Write a matrix of k's as follows:

$$\begin{bmatrix} k_{11} & k_{21} & \dots & k_{n1} \\ k_{12} & k_{22} & \dots & k_{n2} \\ \dots & \dots & \dots & \dots \\ k_{1n} & k_{2n} & \dots & k_{nm} \end{bmatrix}.$$

Now replace each k_{ij} in this matrix by zero if it does not appear in the model. Replace k_{ii} by $-k_i$ on the diagonal and define the k_i to be equal to the sum of the remaining k's in that column.

This study was supported by NIH Grants RG 03545-19 and 5 K06 GM 16,687-10.

References

1. Aceves, J., Erlij, D. 1971. Sodium transport across the isolated epithelium of the frog skin. *J. Physiol.* **212**:195
2. Andersen, B., Zerahn, K. 1963. Method of non-destructive determination of the sodium transport pool in frog skin with radiosodium. *Acta Physiol. Scand.* **59**:319
3. Berridge, M. J., Oshman, J. L. 1972. Transporting Epithelia. Academic Press, Inc., New York and London
4. Biber, T. U. L. 1971. Effect of changes in transepithelial transport on the uptake of sodium across the outer surface of the frog skin. *J. Gen. Physiol.* **58**:131
5. Biber, T. U. L., Chez, R. A., Curran, P. F. 1966. Na transport across frog skin at low external Na concentrations. *J. Gen. Physiol.* **49**:1161
6. Biber, T. U. L., Cruz, L. J., Curran, P. F. 1972. Sodium influx at the outer surface of frog skin. *J. Membrane Biol.* **7**:365
7. Biber, T. U. L., Curran, P. F. 1970. Direct measurement of uptake of sodium at the outer surface of the frog skin. *J. Gen. Physiol.* **56**:83
8. Campbell, J. P., Aiyawar, R. M., Berry, E. R., Huf, E. G. 1967. Electrolytes in frog skin secretions. *Comp. Biochem. Physiol.* **23**:213
9. Cereijido, M., Curran, P. F. 1965. Intracellular electrical potentials in frog skin. *J. Gen. Physiol.* **48**:543
10. Cereijido, M., Herrera, F. C., Flanigan, W. J., Curran, P. F. 1964. The influence of Na concentration on transport across frog skin. *J. Gen. Physiol.* **47**:879
11. Cereijido, M., Reisin, I., Rotunno, C. A. 1968. The effect of sodium concentration on the content and distribution of sodium in frog skin. *J. Physiol.* **196**:237
12. Cereijido, M., Rotunno, C. A. 1967. Transport and distribution of sodium across frog skin. *J. Physiol.* **190**:481
13. Cereijido, M., Rotunno, C. A. 1971. The effect of antidiuretic hormone on Na movement across frog skin. *J. Physiol.* **213**:119
14. Curran, P. F., Herrera, F. C., Flanigan, W. J. 1963. The effect of Ca and antidiuretic hormone on Na transport across frog skin. *J. Gen. Physiol.* **46**:1011
15. Diamond, J. M., Bossert, W. H. 1967. Standing-gradient osmotic flow. A mechanism for coupling of water and solute transport in epithelia. *J. Gen. Physiol.* **50**:2061
16. Dörge, A., Nagel, W. 1970. Effect of amiloride on sodium transport in frog skin. *Pflüg. Arch. Ges. Physiol.* **321**:91
17. Engbaek, L., Hoshiko, T. 1957. Electrical potential gradients through frog skin. *Acta Physiol. Scand.* **39**:348
18. Farquhar, M. G., Palade, G. E. 1964. Functional organization of amphibian skin. *Proc. Nat. Acad. Sci.* **51**:569
19. Farquhar, M. G., Palade, G. E. 1965. Cell junctions in amphibian skin. *J. Cell Biol.* **26**:263
20. Hoshiko, T., Lindley, B. D., Edwards, C. 1964. Diffusion delay in frog skin connective tissue: A source of error in tracer investigations. *Nature* **201**:932
21. Huf, E. G. 1972. The role of Cl^- and other anions in active Na^+ transport in isolated frog skin. *Acta Physiol. Scand.* **84**:366

22. Huf, E. G., Doss, N. S., Wills, J. P. 1957. Effects of metabolic inhibitors and drugs on ion transport and oxygen consumption in isolated frog skin. *J. Gen. Physiol.* **41**:397
23. Hvid-Hansen, H., Zerahn, K. 1964. Concentration of lithium, sodium, and potassium in epithelial cells of the isolated frog skin during active transport of lithium. *Acta Physiol. Scand.* **60**:189
24. Koefoed-Johnsen, V., Ussing, H. H. 1958. Nature of the frog skin potential. *Acta Physiol. Scand.* **42**:298
25. Nagel, W. W., Dörge, A. 1970. Effect of amiloride on sodium transport of frog skin. *Pflüg. Arch. Ges. Physiol.* **317**:84
26. Nagel, W., Dörge, A. 1971. A study of the different sodium compartments and the transepithelial sodium fluxes of the frog skin with the use of ouabain. *Pflüg. Arch. Ges. Physiol.* **324**:267
27. Rotunno, C. A., Vilallonga, F. A., Fernández, M., Cereijido, M. 1970. The penetration of sodium into the epithelium of the frog skin. *J. Gen. Physiol.* **55**:716
28. Salako, L. A., Smith, A. J. 1970*a*. Effects of amiloride on active sodium transport by the isolated frog skin: Evidence concerning site of action. *Brit. J. Pharmacol.* **38**:702
29. Salako, L. A., Smith, A. J. 1970*b*. Changes in sodium pool and kinetics of sodium transport in frog skin produced by amiloride. *Brit. J. Pharmacol.* **39**:99
30. Smith, T. C., Martin, J. H., III, Huf, E. G. 1973. Sodium pool and sodium concentration in epidermis of frog skin. *Biochim. Biophys. Acta* **291**:465
31. Ussing, H. H., Windhager, E. E. 1964. Nature of shunt-path and active sodium transport path through frog skin epithelium. *Acta Physiol. Scand.* **61**:484
32. Voûte, C. L. 1963. An electron microscopic study of the skin of the frog (*Rana pipiens*). *J. Ultrastruct. Res.* **9**:497
33. Voûte, C. L., Ussing, H. H. 1968. Some morphological aspects of active sodium transport. *J. Cell. Biol.* **36**:625
34. Voûte, C. L., Ussing, H. H. 1970. The morphological aspects of shunt-path in the epithelium of the frog skin. (*R. temporaria*). *Exp. Cell Res.* **61**:133
35. Watlington, C. O. 1968. Effect of catecholamines and adrenergic blockade on sodium transport of isolated frog skin. *Amer. J. Physiol.* **214**:1001
36. Watlington, C. O. 1969. α-adrenergic inhibition of Na^+ transport: The interaction of vasopressin and 3′,5′-AMP. *Biochim. Biophys. Acta (Amst.).* **193**:394
37. Watlington, C. O., Huf, E. G. 1971. β-adrenergic stimulation of frog skin mucous glands: Non-specific inhibition by adrenergic blocking agents. *Comp. Gen. Pharmacol.* **2**:295
38. Watlington, C. O., Smith, T. C., Huf, E. G. 1970. Direct electrical currents in metabolizing epithelial membranes. *In*: Experiments in Physiology and Biochemistry. G. A. Kerkut, editor. Vol. 3, p. 49. Academic Press Inc., London and New York
39. Whittembury, G. 1964. Electrical potential profile of the toad skin epithelium. *J. Gen. Physiol.* **47**:795
40. Winn, P. M., LaPrade, N. S., Tolbert, W. R., Huf, E. G. 1966. On the nature of the resting frog skin potential. *Medical College of Virginia Quart.* **2**:116
41. Winn, P. M., Smith, T. C., Campbell, A. D., Huf, E. G. 1964. Sodium diffusion in epidermis and corium of frog skin and in Ringer-agar gel. *J. Cell Comp. Physiol.* **47**:795
42. Zerahn, K. 1956. Oxygen consumption and active sodium transport in the isolated and short-circuited frog skin. *Acta Physiol. Scand.* **36**:300
43. Zerahn, K. 1969. Nature and localization of the sodium pool during active transport in the isolated frog skin. *Acta Physiol. Scand.* **77**:272